

Superconductivity at 22.3 K in $\text{SrFe}_{2-x}\text{Ir}_x\text{As}_2$

Fei Han, Xiyu Zhu, Ying Jia, Lei Fang, Peng Cheng, Huiqian Luo, Bing Shen and Hai-Hu Wen*

National Laboratory for Superconductivity, Institute of Physics and Beijing National Laboratory for Condensed Matter Physics, Chinese Academy of Sciences, P. O. Box 603, Beijing 100190, China

By substituting the Fe with the 5d-transition metal Ir in SrFe_2As_2 , we have successfully synthesized the superconductor $\text{SrFe}_{2-x}\text{Ir}_x\text{As}_2$ with $T_c = 22.3$ K at $x = 0.5$. X-ray diffraction indicates that the material has formed the ThCr_2Si_2 -type structure with a space group I4/mmm . The temperature dependence of resistivity and dc magnetization both reveal sharp superconducting transitions. An estimate on the diamagnetization signal indicates a high Meissner shielding volume. Interestingly, the normal state resistivity exhibits a roughly linear behavior starting just above T_c all the way up to 300 K. The superconducting transitions at different magnetic fields were also measured yielding a slope of $-dH_{c2}/dT = 3.8$ T/K near T_c . Using the Werthamer-Helfand-Hohenberg (WHH) formula $H_{c2} = -0.69(dH_{c2}/dT)|_{T_c}T_c$, the upper critical field at zero K is found to be about 58 T. Counting the possible number of electrons doped into the system in $\text{SrFe}_{2-x}\text{Ir}_x\text{As}_2$, we argue that the superconductivity in the Ir-doped system cannot be reconciled with the Co-doped case based on a simple rigid band model, which should add more ingredients to understanding the underlying physics of the iron pnictide superconductors.

PACS numbers: 74.70.Dd, 74.25.Fy, 75.30.Fv, 74.10.+v

Since the discovery of superconductivity in $\text{LaFeAsO}_{1-x}\text{F}_x$ ¹, the FeAs-based superconductivity has stimulated great interests in the fields of condensed matter physics and material science. In the ZrCuSiAs structure, the T_c has been quickly promoted to 55-56 K^{2,3} in fluorine doped or oxygen deficient oxy-pnictides REFeAsO (RE = rare earth elements) and rare earth elements doped fluoride-arsenide AeFeAsF (Ae = Ca, Sr) compounds^{4,5}. Later on, in the system of $(\text{Ba}, \text{Sr})_{1-x}\text{K}_x\text{Fe}_2\text{As}_2$ with the ThCr_2Si_2 -type structure (denoted as FeAs-122), the maximum T_c at about 38 K was discovered^{6,7,8}. This FeAs-122 phase provides us a great opportunity to investigate the intrinsic physical properties since large scale crystals can be grown.⁹ Furthermore, it was found that a substitution of Fe ions with Co can also induce superconductivity with maximum T_c of about 24 K^{10,11}. Meanwhile, Ni substitution at Fe site in BaFe_2As_2 has also been carried out with a T_c of 20.5 K¹². Very recently, superconductivity in Ru substituted $\text{BaFe}_{2-x}\text{Ru}_x\text{As}_2$ was found¹³. This indicates that, the superconductivity can be induced by substituting the Fe with not only the 3d-transition metals, such as Co and Ni, but also the 4d metal, like Ru. In this Communication, we report the successful fabrication of the new superconductor $\text{SrFe}_{2-x}\text{Ir}_x\text{As}_2$ with a T_c of about 22 K by replacing the Fe with the 5d-transition metal Ir. X-ray diffraction pattern (XRD), resistivity, DC magnetic susceptibility and upper critical field have been determined on this Ir-doped superconductor. Our discovery here will add extra ingredients in understanding the underlying physics in the iron pnictide superconductors.

The polycrystalline samples $\text{SrFe}_{2-x}\text{Ir}_x\text{As}_2$ were synthesized by using a two-step solid state reaction method¹⁴. Firstly, SrAs, FeAs and IrAs₂ powders were obtained by the chemical reaction method with Sr pieces, Fe powders (purity 99.99%), Ir powders (purity 99.99%)

and As grains. Then they were mixed together in the formula $\text{SrFe}_{2-x}\text{Ir}_x\text{As}_2$, ground and pressed into a pellet shape. All the weighing, mixing and pressing procedures were performed in a glove box with a protective argon atmosphere (both H₂O and O₂ are limited below 0.1 ppm). The pellet was sealed in a silica tube with 0.2 bar of Ar gas and followed by heat treatment at 900 °C for 50 hours. Then it was cooled down slowly to room temperature. A second sintering by repeating above process normally can improve the purity of the sample.

The x-ray diffraction measurement was performed at room temperature using an MXP18A-HF-type diffractometer with Cu-K_α radiation from 10° to 80° with a step of 0.01°. The analysis of x-ray powder diffraction data was done by using the software of Powder-X,¹⁵ and the lattice constants were derived (see below). The DC magnetization measurement was carried out on a superconducting quantum interference device (SQUID) magnetometer (Quantum Design MPMS-7T). In order to remove the effect given by the possible residual magnetic field of the magnet, before the measurement the system was degaussed. In this case the residual magnetic field is limited below 1 Oe. The resistivity measurements were done in a physical property measurement system (Quantum Design, PPMS-9T) with magnetic fields up to 9 T. The six-lead method was used in the measurement on the longitudinal and transverse resistivity at the same time. In this paper we report only the resistivity data and leave other transport properties to be published elsewhere. The temperature stabilization during the measurement was better than 0.1% and the resolution of the voltmeter was better than 10 nV.

In Figure. 1 we present the x-ray diffraction patterns of $\text{SrFe}_{1.5}\text{Ir}_{0.5}\text{As}_2$. The main peaks can be indexed by a tetragonal structure with $a = b = 3.95\text{Å}$ and $c = 12.22\text{Å}$. In the parent phase SrFe_2As_2 ,¹⁶ the lattice constants a (or b) = 3.92 Å, $c = 12.36\text{Å}$. Therefore by doping Ir into

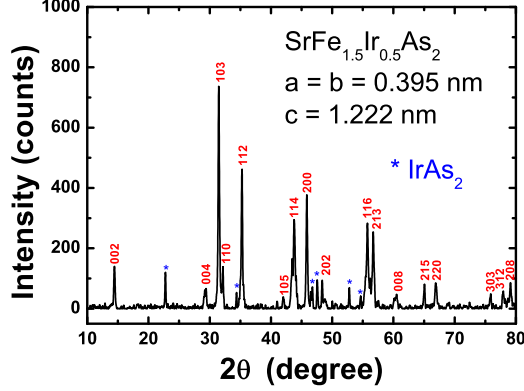


FIG. 1: (Color online) X-ray diffraction patterns for the sample $\text{SrFe}_{1.5}\text{Ir}_{0.5}\text{As}_2$. Almost all main peaks can be indexed by a tetragonal structure with $a = b = 3.95\text{\AA}$ and $c = 12.22\text{\AA}$. The asterisks mark the peaks arising from the impurity phase (most probably the IrAs_2).

the Fe site, the lattice constant a shrinks a bit, while c expands slightly. This tendency is similar to the case of doping potassium to the sites of Ba in $\text{Ba}_{1-x}\text{K}_x\text{Fe}_2\text{As}_2$, or substituting the Fe with Ru in $\text{BaFe}_{2-x}\text{Ru}_x\text{As}_2$.¹³ There are still some small peaks which are coming from the secondary phase, as marked by the asterisks. Further analysis indicates that this tiny amount of impurity is most probably given by IrAs_2 since other peaks with asterisks can be indexed to the structural data of IrAs_2 . Concerning the very large Meissner shielding volume as shown below, the XRD data here shows no doubt that the superconductivity arises from the $\text{SrFe}_{1.5}\text{Ir}_{0.5}\text{As}_2$ phase. We should mention that the composition of Ir here gives only the nominal value. A detailed analysis of the true composition on the grains is under way. In addition, above the nominal doping level of $x=0.5$, we found that the samples fabricated so far contained much more impurity phases. A further refinement on the sample purity at a high doping is strongly desired to illustrate the phase diagram of the system.

In Figure. 2 we present the temperature dependence of DC magnetization for the sample $\text{SrFe}_{1.5}\text{Ir}_{0.5}\text{As}_2$. The measurement was carried out under a magnetic field of 20 Oe in zero-field-cooled and field-cooled processes. A clear diamagnetic signal appears below 20.7 K, which corresponds to the middle transition temperature of the resistivity data. A very strong Meissner shielding signal was observed in the low temperature regime. Considering the shape of the sample (round disc with a diameter of 5 mm and thickness of 1.3 mm), the Meissner shielding volume is close to be full. We should mention that due to the uncertainty in counting the demagnetization factor, it is difficult to calculate the precise volume of the Meissner shielding. However, the strong diamagnetization value is found to be among the strongest magne-

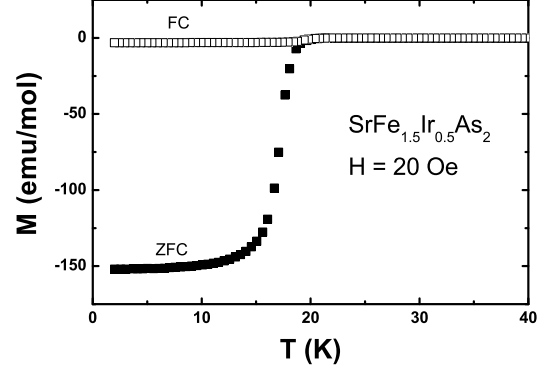


FIG. 2: (Color online) Temperature dependence of DC magnetization for the sample $\text{SrFe}_{1.5}\text{Ir}_{0.5}\text{As}_2$. The measurement was done under a magnetic field of 20 Oe in zero-field-cooled and field-cooled modes. A strong Meissner shielding signal was observed here.

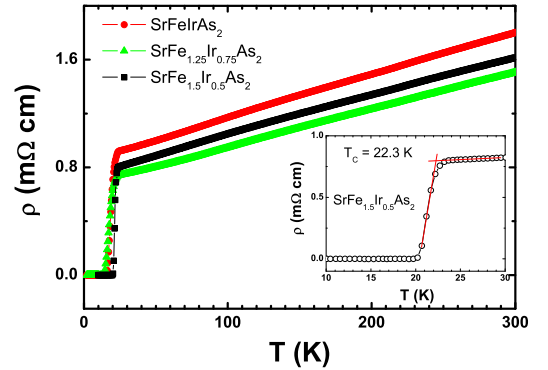


FIG. 3: (Color online) Temperature dependence of resistivity for sample $\text{SrFe}_{2-x}\text{Ir}_x\text{As}_2$ ($x = 0.5, 0.75, 1$). The T_c value here for the sample with $x=0.5$ was determined with a classical method, i.e., the crossing point of the normal state background and the extrapolation of the most steep transition part. A roughly linear temperature dependence in the whole temperature region is obvious.

tization (in emu/mol) found so far in the iron pnictide superconductors, which signals a rather large volume of superconductivity in the present sample.

Figure. 3 shows the temperature dependence of resistivity for samples $\text{SrFe}_{2-x}\text{Ir}_x\text{As}_2$ with $x = 0.5, 0.75$ and 1, respectively. It was shown that the parent phase exhibits a sharp drop of resistivity (resistivity anomaly as called so far) at about 205 K.¹⁷ However in our superconducting samples, this anomaly disappeared completely. The sample with nominal composition $x=0.5$ shows a superconducting transition at about 22.3 K which is determined by a classical method, i.e., the crossing point of the normal state background and the extrapolation of

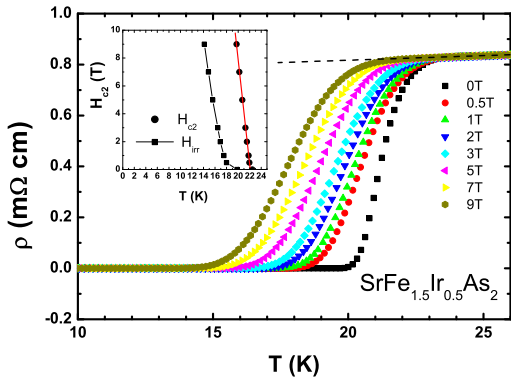


FIG. 4: (Color online) Temperature dependence of resistivity for sample $\text{SrFe}_{1.5}\text{Ir}_{0.5}\text{As}_2$ at different magnetic fields. The dashed line indicates the extrapolated resistivity in the normal state. One can see that the superconductivity seems to be robust against the magnetic field and shifts slowly to the lower temperatures. The inset gives the upper critical field determined using the criterion of $90\%\rho_n$. A slope of $-dH_{c2}/dT = 3.8 \text{ T/K}$ near T_c is found here. The irreversibility line H_{irr} taking with the criterion of $0.1\% \rho_n$ is also presented in the inset.

the transition part with the most steep slope. The transition width determined here with the criterion of $10-90\% \rho_n$ is about 1.8 K with ρ_n the normal state resistivity (as marked by the dashed line Fig.3). With higher doping ($x=0.75$ and 1.0) the transition temperature declines slightly. As mentioned before, the samples with higher doping levels ($x=0.75$ and 1.0) contain much more impurities, therefore we are not sure whether this slight drop of superconducting transition temperature is due to the chemical phase separation or it is due to the systematic evolution of T_c vs. doping level. Interestingly, the normal state resistivity of the superconducting sample $x=0.5$ shows a roughly linear behavior starting just above T_c all the way up to 300 K . It is certainly illusive to know whether this linear behavior keeps going down to very low temperatures when the superconductivity is suppressed by the strong magnetic field. Further efforts are worthwhile to unravel whether this linearity reflects an intrinsic feature of a novel electron scattering. Since the sample with $x=0.5$ shows already a reliable quality, we would believe that this linear temperature dependence of resistivity is intrinsic and may possess itself of great importance. More data are desired to clarify this interesting feature in the normal state, together with the systematic evolution of the superconducting properties by doping Ir.

In Fig.4 we present the temperature dependence of resistivity under different magnetic fields. Just as many other iron pnictide superconductors, the superconductivity is very robust against the magnetic field in the present sample. We used the criterion of $90\%\rho_n$ to determine the upper critical field and show the data in the inset of

Fig.4. A slope of $-dH_{c2}/dT = 3.8 \text{ T/K}$ can be obtained here. This is a rather large value which indicates a rather high upper critical field in this system. In order to determine the upper critical field in the low temperature region, we adopted the Werthamer-Helfand-Hohenberg (WHH) formula¹⁸ $H_{c2} = -0.69(dH_{c2}/dT)|_{T_c}T_c$. Taking $dH_{c2}/dT|_{T_c} = -3.8 \text{ T/K}$ and $T_c = 22.3 \text{ K}$, we have $H_{c2}(0) = 58 \text{ T}$. This indicates that the present Ir-doped sample has also a very large upper critical field, as in K-doped¹⁹ and Co-doped samples.²⁰ Very recently the high upper critical fields, as a common feature in the iron pnictide superconductors, were interpreted as due to the strong disorder effect.²¹

The superconductivity induced by doping Co in $(\text{Ba,Sr})(\text{Fe}_{1-x}\text{Co}_x)_2\text{As}_2$ can be understood that electrons are introduced into the system, which suppresses the antiferromagnetic order.²² It was reported that the maximum superconducting transition T_c in the Co-doped system is about 24 K which occurs at the doping level of $x = 0.08$.^{23,24} Assuming the Co ions in this sample have valence state of 3^+ , therefore the optimized superconductivity takes place when $0.08/\text{Fe}$ electrons are doped into the sample. When the doping level is about $0.16/\text{Fe}$, it was found that the superconductivity disappeared in the Co-doped case.^{23,24} In the present case with Ir-doping, this scenario seems inapplicable. The usual valence state of Ir element in an oxide is 4^+ , the superconducting sample with $x=0.5$ in $\text{SrFe}_{2-x}\text{Ir}_x\text{As}_2$ corresponds to a doping level of 0.5-electron/Fe , this is already far beyond the value of $0.16/\text{Fe}$ in achieving superconductivity with Co-doping. Therefore the superconductivity in the Co-doped and Ir-doped cases cannot be reconciled by a consideration based on the rigid band model. A band structure calculation to such a high doping level in the Ir-doped case is strongly recommended. In addition, the outer shell of Ir^{4+} ion has 5 electrons left, which is an odd number and is different from the cases of Fe^{2+} (6 electrons), Ni^{2+} (8 electrons) and Co^{3+} (6 electrons). Therefore it is a poorly footed argument that the superconductivity occurs only in the system with even electrons in the outer shell of the ions. Furthermore the electrons of the 5d transition metals have higher itinerancy than the 3d ones. In a naive picture, it would suggest that the higher itinerancy of the doped electrons in the Ir-doped sample may lead to the superconductivity. All these interesting hypothesis concerning the superconductivity in our Ir-doped samples put more ingredients to understanding the underlying physics of the pnictide superconductors.

In summary, superconductivity with $T_c = 22.3 \text{ K}$ has been observed in $\text{SrFe}_{1.5}\text{Ir}_{0.5}\text{As}_2$. The normal state resistivity exhibits a roughly linear behavior starting just above T_c all the way up to 300 K . This may reflect a novel scattering mechanism in the normal state. The superconductivity is rather robust against the magnetic field with a slope of $-dH_{c2}/dT = 3.8 \text{ T/K}$ near T_c . Using the Werthamer-Helfand-Hohenberg (WHH) formula $H_{c2} = -0.69(dH_{c2}/dT)|_{T_c}T_c$, we got the upper critical field at zero K of about 58 T . Based on the estimate

on the high electron density (0.5-electron/Fe) in the Ir-doped superconducting sample, we argue that the superconductivity induced by doping Ir and Co cannot be reconciled with the simple rigid band model.

This work is supported by the Natural Science Foundation of China, the Ministry of Science and Technology of China (973 project: 2006CB601000, 2006CB921802),

the Knowledge Innovation Project of Chinese Academy of Sciences (ITSNEM).

References

-
- * Electronic address: hhwen@aphy.iphy.ac.cn
- ¹ Y. Kamihara, T. Watanabe, M. Hirano, and H. Hosono, *J. Am. Chem. Soc.* **130**, 3296 (2008).
 - ² Z. A. Ren, W. Lu, J. Yang, W. Yi, X. L. Shen, Z. C. Li, G. C. Che, X. L. Dong, L. L. Sun, F. Zhou, and Z. X. Zhao, *Chin. Phys. Lett.* **25**, 2215 (2008).
 - ³ C. Wang, L. Li, S. Chi, Z. Zhu, Z. Ren, Y. Li, Y. Wang, X. Lin, Y. Luo, S. Jiang, X. Xu, G. Cao, Z. Xu, *Europhys. Lett.* **83**, 67006 (2008).
 - ⁴ X. Zhu, F. Han, P. Cheng, G. Mu, B. Shen, and H. H. Wen, *Europhys. Lett.* **85**, 17011 (2009).
 - ⁵ P. Cheng, B. Shen, G. Mu, X. Zhu, F. Han, B. Zeng, and H. H. Wen, *arXiv:cond-mat/0812.1192* (2008), *EPL*, in press.
 - ⁶ M. Rotter, M. Tegel, I. Schellenberg, W. Hermes, R. Pottgen, and D. Johrendt, *Phys. Rev. B* **78**, 020503(R) (2008).
 - ⁷ M. Rotter, M. Tegel, and D. Johrendt, *Phys. Rev. Lett.* **101**, 107006 (2008).
 - ⁸ K. Sasmal, B. Lv, B. Lorenz, A. Guloy, F. Chen, Y. Xue, and C. W. Chu, *Phys. Rev. Lett.* **101**, 107007 (2008).
 - ⁹ N. Ni, S. L. Bud'ko, A. Kreyssig, S. Nandi, G. E. Rustan, A. I. Goldman, S. Gupta, J. D. Corbett, A. Kracher, P. C. Canfield, *Phys. Rev. B* **78**, 014507 (2008).
 - ¹⁰ A. S. Sefat, R. Jin, M. A. McGuire, B. C. Sales, D. J. Singh, and D. Mandrus, *Phys. Rev. Lett.* **101**, 117004 (2008).
 - ¹¹ Y. K. Li, X. Lin, Z. W. Zhu, H. Chen, C. Wang, L. J. Li, Y. K. Luo, M. He, Q. Tao, H. Y. Li, G. H. Cao, Z. A. Xu, *Phys. Rev. B* **79**, 054521 (2009).
 - ¹² L. J. Li, Q. B. Wang, Y. K. Luo, H. Chen, Q. Tao, Y. K. Li, X. Lin, M. He, Z. W. Zhu, G. H. Cao, and Z. A. Xu, *arXiv:cond-mat/0809.2009* (2008).
 - ¹³ S. Paulraj, S. Sharma, A. Bharathi, A. T. Satya, S. Chandra, Y. Hariharan, and C. S. Sundar, *arXiv:cond-mat/0902.2728* (2009).
 - ¹⁴ X. Zhu, H. Yang, L. Fang, G. Mu, and H. H. Wen, *Supercond. Sci. Technol.* **21**, 105001 (2008).
 - ¹⁵ C. Dong, *J. Appl. Cryst.* **32**, 838 (1999).
 - ¹⁶ M. Tegel, M. Rotter, V. Weiss, F. M. Schappacher, R. Pottgen, D. Johrendt, *J. Phys.: Condens. Matter* **20**, 452201 (2008).
 - ¹⁷ C. Krellner, N. Caroca-Canales, A. Jesche, H. Rosner, A. Ormeci, C. Geibel, *Phys. Rev. B* **78**, 100504(R), 2008.
 - ¹⁸ N. R. Werthamer, E. Helfand, P. C. Hohenberg, *Phys. Rev.* **147**, 295 (1966).
 - ¹⁹ Z. S. Wang, H. Q. Luo, C. Ren, H. H. Wen, *Phys. Rev. B* **78**, 140501(R) (2008).
 - ²⁰ Y. J. Jo, J. Jaroszynski, A. Yamamoto, A. Gurevich, S. C. Riggs, G. S. Boebinger, D. Larbalastier, H. H. Wen, N. D. Zhigadlo, S. Katrych, Z. Bukowski, J. Karpinski, R. H. Liu, H. Chen, X. H. Chen, L. Balicas, *arXiv:cond-mat/0902.0532* (2009).
 - ²¹ G. Fuchs, S. L. Drechsler, N. Kozlova, M. Bartkowiak, G. Behr, K. Nenkov, H. H. Klauss, H. Maeter, A. Amato, H. Luetkens, A. Kwadrin, R. Khasanov, J. Freudenberger, A. Koehler, M. Knupfer, E. Arushanov, B. Buechner, L. Schultz, *arXiv:cond-mat/0902.3498* (2009).
 - ²² C. De la Cruz, Q. Huang, J. W. Lynn, J. Li, I. W. Ratcliff, J. L. Zarestky, H. A. Mook, G. F. Chen, J. L. Luo, N. L. Wang and P. Dai, *Nature* **453**, 899 (2008).
 - ²³ N. Ni, M. E. Tillman, J.-Q. Yan, A. Kracher, S. T. Hannahs, S. L. Bud'ko, P. C. Canfield, *Phys. Rev. B* **78**, 214515 (2008).
 - ²⁴ J.-H. Chu, J. G. Analytis, C. Kucharczyk and I. R. Fisher, *Phys. Rev. B* **79**, 014506 (2009).